DOI: 10.1002/
Article type: Communication

Title: Microfluidic Mass Production of Stabilized and Stealthy Liquid Metal Nanoparticles

Shi-Yang Tang, Ruirui Qiao, Sheng Yan, Dan Yuan, Qianbin Zhao, Guolin Yun, Thomas P. Davis*, and Weihua Li**

S.-Y. Tang and R. Qiao made equal contribution to this work

Dr. S.-Y. Tang, Dr. S. Yan, D. Yuan, Q. Zhao, G. Yun, Prof. W. Li
School of Mechanical, Materials, Mechatronic and Biomedical Engineering, University of Wollongong, Australia
E-mail: shiyang@uow.edu.au; weihuali@uow.edu.au

Dr. R. Qiao, Prof. T. P. Davis
ARC Centre of Excellence in Convergent Bio-Nano Science and Technology, Drug Delivery, Disposition and Dynamics Theme, Monash Institute of Pharmaceutical Sciences, Monash University, Parkville, VIC 3052, Australia
E-mail: thomas.p.davis@monash.edu

Prof. T. P. Davis
Department of Chemistry, University of Warwick, Gibbet Hill, Coventry CV4 7AL, United Kingdom

Keywords: Microfluidics; EGaIn; Liquid metal; Nanoparticle; Acoustics

Abstract:

Functional nanoparticles comprised of liquid metals, such as eutectic gallium indium (EGaIn) and Galinstan, present exciting opportunities in the fields of flexible electronics, sensors, catalysts, and drug delivery systems. Methods used currently for producing liquid metal nanoparticles have significant disadvantages as they rely on both bulky and expensive high-power sonication probe systems, and also generally require the use of small molecules bearing thiol groups to stabilize the nanoparticles. Herein, we describe an innovative microfluidics-enabled platform as an inexpensive, easily accessible method for the on-chip mass production of EGaIn nanoparticles with tunable size distributions in an aqueous medium. We also report a novel nanoparticle-stabilization approach using brushed polyethylene glycol chains with trithiocarbonate end-groups negating the requirements for thiol additives whilst imparting a 'stealth' surface layer. Furthermore, we demonstrate a surface modification of the nanoparticles using galvanic replacement, and conjugation with antibodies. We envision that the demonstrated microfluidic technique can be used as an economic and versatile platform for the rapid production of liquid metal-based nanoparticles for a range of biomedical applications.

EGaIn and Galinstan are promising alternatives to mercury due to their negligible vapor pressure and low-toxicity,[1] and many applications have been suggested for such gallium-based liquid metals especially in the fields of microfluidic systems[2] and soft electronics.[3] 'Bottom-up' methods are most commonly used to synthesize nanoparticles via the nucleation and growth of particles from fine molecular distributions in liquid or vapor phases.[4] In contrast, gallium-based eutectic liquid metal alloys, such as eutectic gallium indium (EGaIn, m.pt. 15.5 °C) and gallium indium tin (Galinstan, m.pt. −19 °C), optimally form nanoparticles following a "top-down" method. Disruptive forces induced by acoustic or microfluidic devices have been utilized for overcoming the surface tension of bulk EGaIn and Galinstan liquid metals to form micro/nano-size particles within liquid phases. The rapid formation of a thin oxide layer on the surface of particulate liquid metals helps prevent coalescence back to the bulk materials.[5] Due to its superior electrical properties such as high conductivity and high hydrogen overpotential, numerous applications based on droplets of liquid metals have been explored including chemical sensors and soft circuit elements.[5b,5c] In addition, the presence of the oxide layer allows for the formation of liquid metal/metal oxide (LM/MO) frameworks, making the liquid metal particles useful for photocatalytic applications.[6] More importantly, such liquid metal nanoparticles are transformable upon the application of external stimuli such as change of pH and temperature, their application of smart drug delivery systems with a promoted drug releasing performance have recently been studied.[5d,7]

High-power sonication probe systems have been commonly applied to induce acoustic forces for disrupting bulk liquid metals into nanoparticles.[5b,5d,5e,7a] In addition, micro to nano-sized EGaIn particles can also be produced using the droplet emulsion technique by shearing the liquid metal using a rotary tool in the presence of a carrier fluid.[8] In comparison to ultrasonic bath, sonication

probe is able to produce a much larger power density and therefore, yielding a much higher efficiency for producing nanoparticles.[6c] However, sonication probe can lead to rapid heating induced by the intense power density, driving undesired oxidation, dealloying, and transformation processes of the liquid metal nanoparticles.[5e,6a,6c] Ideally, important parameters such as the size distribution of the nanoparticles should be controlled and modulated by changing power and sonication time. In practice, process dependent parameters are often just as influential on the product outcome, such as the position of the sonication probe, volume of liquid and reactor dimensions. Microfluidic systems possesses many advantages including low reagent consumption; precise control over process parameters such as flow velocity, shear stress, heat/mass transfer, and concentration of chemicals in microscale; as well as allowing for streamlined process by integrating multi-steps on a single chip, making them very useful for modulating critical stages required to produce nanoparticles in a highly controlled manner.[9] Moreover, thiolated small molecules or thiol compounds (molecular weight, MW $\leq$ 1000) are often used to stabilize the final liquid metal nanoparticles.[5d,10] Unfortunately, thiol groups have an unpleasant smell, are prone to oxidation, and often not suitable for direct use in biological systems as they foul readily.[11]

Therefore, we have been impelled to design a manufacturing process that is simple, highly reproducible, inexpensive, small but easily scalable, and suitable for the production of stable and stealthy liquid metal nanoparticles. Consequently, we now report on an innovative microfluidics-based system for efficiently producing EGaIn nanoparticles in aqueous media using a conventional ultrasonic bath. We also report on the use of trithiocarbonate-functionalized brushed polyethylene glycol (bPEG) with molecular weights of 5 to 20 kDa to graft the produced nanoparticles for imbuing both stability and stealth properties. Finally, we report on the

modification and bio-functionalization of the surface of EGaIn nanoparticles using contiguous processes of galvanic replacement and antibody conjugation.

The microfluidic manufacturing system is illustrated in **Figure 1**A. The polydimethylsiloxane (PDMS) microchannel is plasma treated and bonded onto a thin glass slide (24 × 50 × 0.1 mm) and immobilized using a polymethyl methacrylate (PMMA) holder. The role of the PMMA holder was to prevent any movement of the microchannel induced by acoustic waves during particle processing. The microfluidic chip has a T-junction with a width and height *H* of 500 and 50 μm, respectively, connected to a serpentine shaped channel with a width *W* and length *L* of 5 and 50 mm, respectively, as shown in the lower-left inset of Fig. 1A. The assembled system is illustrated in the upper-left inset of Fig. 1A. After construction, the integrated system was placed into an ultrasonic bath, as shown in Fig. 1B. The 1.3 L ultrasonic bath used in our study was equipped with a 65 W ultrasonic transducer set at a resonant frequency of 20 kHz. The tank was filled with 500 mL water and the microchannel was placed on the top of the transducer. The temperature of the water was maintained below 35˚C. Two syringe pumps were used for injecting the suspension medium and EGaIn into the T-junction, a 1.5 mL test tube was then used for collecting the product suspension at the outlet (Fig. 2B). The cross-sectional view of the overall setup is given in Fig. 1C, in which it is evident that the thin glass slide is in intimate contact with the base of the tank thereby maximizing acoustic energy transferred into the microchannel to ensure optimal nanoparticle production efficiency.

A scheme illustrating the process of EGaIn nanoparticle production is shown in Fig. 1D. The T-junction is widely used in microfluidics for producing microdroplets. However, EGaIn poses an extra challenge in microfluidics because of its large surface tension relative to water, that creates a significant barrier to microdroplet formation unless a high-viscous liquid is used.[5a] In this

work, we synthesized bPEG polymers with molecular weights of 5 and 20 kDa using reversible addition–fragmentation chain transfer (RAFT) polymerization method to coat and stabilize the nanoparticles,[12] as detailed in Supporting Information S1. We used a bPEG (MW 5 kDa) solution with a concentration of 500 μM as the continuous phase at a dilution that minimized viscosity effects. We initially demonstrated that, EGaIn cannot be broken into microparticles at the T-junction even when a high flow rate ratio of 50 between the continuous and discrete phases was applied, as shown in Supporting Information S2. Consequently, we designed experiments to utilize additional oscillating shear forces induced by ultrasonic acoustic waves to break the bulk EGaIn into microdroplets at the T-junction, and subsequently to disrupt the particles further to nano-sizes when flowing through the microchannel towards the outlet (Fig. 1D). The experimental results are illustrated in Fig. 1E, showing snapshots from a high-speed video clearly showing the production of EGaIn microdroplets at the T-junction when the flow rates of the bPEG solution and EGaIn were set at 50 and 1 μL/min, respectively. The formed microdroplets rapidly disrupted into smaller particles with the application of acoustic waves (also see Movie S1). This process produced a colloidal suspension containing a high concentration of EGaIn nanoparticles and the downstream microchannel exhibited opacity (Fig. 1E). Since the suspended nanoparticles are only exposed to high ultrasonic energy inside the microchannel for ~15 s before exiting the outlet, our system minimizes the chance for inducing dealloying and morphological transformation processes observed for EGaIn nanoparticles within aqueous media caused by oxidation of gallium metal due to the prolonged (> 5 min) exposure to high temperature (~70 °C).[5e,6a,6c]

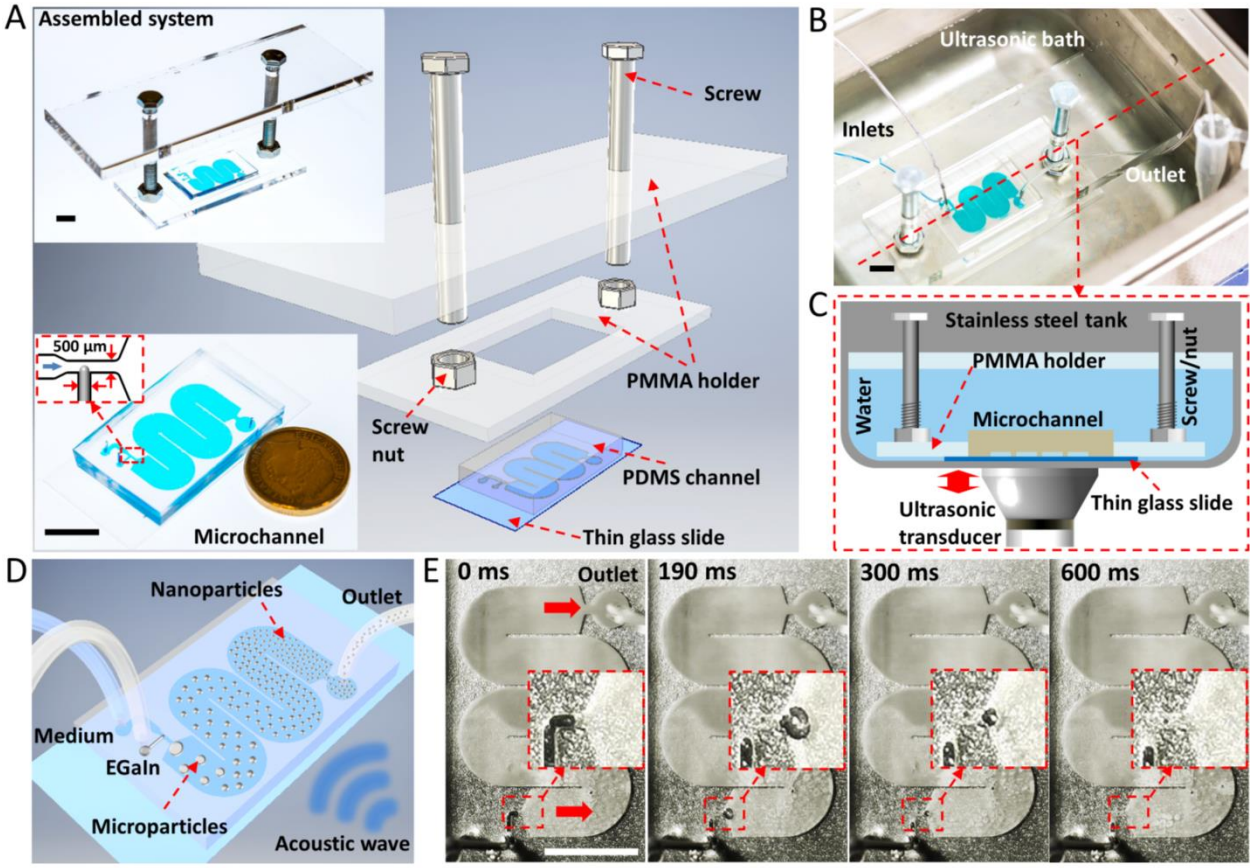

Figure 1. Experimental setup of the on-chip nanoparticle production platform and its working mechanism. (A) Exploded schematic of the platform for on-chip production of liquid metal nanoparticles, the upper inset shows the assembled system, and the lower inset shows the microfluidic chip with a T-junction. (B) The assembled system is placed in a sonication bath, in which bulk liquid metal is broken into nanoparticles to form a colloidal suspension. (C) Schematic of the cross-sectional view of the entire system. (D) Schematic of the working mechanism, where liquid metal microdroplets are formed at the T-junction with the presence of acoustic waves, and later gradually broken into nanoparticles when travelling along the microchannel. (E) Snap shots taken from a high-speed camera showing the formation and breaking down of a microdroplet to form nanoparticles within the microchannel. Scale bar is 1 cm.

The bPEG polymers used in this work have a brush-like structure with carboxyl and trithiocarbonate termini. PEG chains have been widely used in nanoparticle engineering for improving stability, biocompatibility and imbuing an anti-biofouling coating to nanoparticles.[13] bPEG has some advantages over linear PEG as macromolecular structural features can be easily controlled using the versatility of living radical polymerization.[14] bPEG can also yield high grafting densities and can thus be advantageous in inducing stability and biocompatibility to nanoparticles. The proposed scheme for the interaction between bPEG and an EGaIn nanoparticle is depicted in **Figure 2**A, where the trithiocarbonate groups attach to the surface of EGaIn, forming a conjugated system to anchor bPEG chains on the surface of the liquid metal similar to the case reported for grafting gold nanoparticles using polymers with trithiocarbonate groups. [15]

Using the microfluidic platform given in Fig. 1, bPEG grafted EGaIn nanoparticles with sizes ranging from tens to a few hundreds of nanometers were produced, as shown by the scanning electron microscopy (SEM) data given in Fig. 2B. The produced nanoparticles were washed with DI water prior to SEM analyses. We conducted a control experiment using a glass vial for producing EGaIn particles utilizing the same bPEG polymer solution (i.e. in the absence of microfluidics). After 10 min sonication EGaIn particles were observed larger than 1 μm diameters, similar to the previously reported results,[6c] only a very small subset of liquid metal was disrupted into submicron or nano-sized particles, as shown in the Supporting Information S3. The insets of Fig. 2B show the EGaIn nanoparticle colloidal suspensions obtained using both the microfluidic chip and the glass vial after removing larger particles using a centrifuge (800 RPM for 15 s). It is evident that the color of the suspension obtained from the microchannel is significantly darker than the one produced from the static glass vial experiment, indicating that a

much higher yield of nanoparticle (measured concentration of ~50 mg/mL) was obtained using the microchannel when compared to the result achieved from the glass vial (~3 mg/mL). The significant enhancement of the nanoparticle production efficiency in a microchannel can be attributed to a number of factors including 1) the thin glass slide used in the experiment can transfer the acoustic energy from the transducer under the microchannel efficiently with less energy loss, and 2) the acoustic impedance mismatching between the bPEG solution and the PDMS further confines the acoustic energy within the microchannel to yield a much higher energy density, enabling the efficient induction of more severe vortices to break the liquid metal into smaller nanoparticles.

The surface of EGaIn nanoparticles is relatively smooth in the absence of bPEG, as shown in the transmission electron microscope (TEM) images given in Fig. 2C taken for the nanoparticles obtained when using DI water as the suspending medium. An oxide layer with a thickness of ~4 nm was observed on the surface of the EGaIn nanoparticles (Fig. 2C). Given that the oxide layer may grow with time due to the diffusion of oxygen,[16] our results from the convergent-beam electron diffraction (CBED) measurement clearly proof the liquidity of the cores for EGaIn nanoparticles with the diameters larger than 30 nm, as given in Supporting Information S4. Interestingly, we observed a uniform coating of bPEG on the surface of the particles in the TEM images given in Fig. 2D when bPEG solution was utilized for producing nanoparticles. Such bPEG coatings can also be observed in the SEM images given in Fig. 2B, and were further evidenced by the X-ray photoelectron spectroscopy (XPS) spectrum obtained for the EGaIn nanoparticles shown in Fig. 2E; peaks of Ga 2p, In 3d, O 1s, C 1s, and S 2p were detected, and the peaks of C 1s and S 2p could be contributed by the bPEG polymer coating. The inset of Fig. 2E shows the magnified spectrum for the S 2p peak. Interestingly, only one peak at ~163.5 eV for

C─S bond was observed without the presence of the peak at ~162 eV for C=S bond;[17] this is probably due to the formation of surface interactions (see Fig. 2A), where the signals for the sulfur atoms interacting with the liquid metal surface overlap with the C─S bond not interacting with the liquid metal. We further conducted energy-dispersive X-ray spectroscopy (EDS) mapping for a single and a cluster of the produced nanoparticles to show the distribution of gallium, indium, oxygen, and sulfur, as well as the presence of oxide and bPEG layers on their surface, as shown in Supporting Information S5.

The hydrodynamic size *D* of the EGaIn nanoparticles was measured using a dynamic light scattering (DLS) system and the data is given in Fig. 1F; the peak size is found at ~400 nm, and the average size of the produced nanoparticles is ~350 nm. We conducted a series of experiments to examine the stability of the product nanoparticles in aqueous based solutions, as shown in Fig. 2G. We found that the nanoparticles are unstable and quickly aggregate in DI water, precipitating onto the bottom of the test tube only 1 h post-production. In addition, the yield of the nanoparticle production is low in DI water (~4 mg/mL) due to their rapid aggregation, and therefore, a smaller yield of nanoparticles could be suspended after centrifuging. In contrast, the yield of EGaIn nanoparticles is much higher when using bPEG polymer (MW of 5 kDa) solution at a concentration of 500 μM (Fig. 2G). We found that the nanoparticle suspension was more stable when using bPEG with a larger molecular weight (20 kDa), and this was corroborated by minimal nanoparticle precipitation 48 hours after production when compared to similar experiments using bPEG with a MW of 5 kDa (Fig. 2G). When we conducted the DLS measurements on the suspensions 48 h after production, we observed a change in the hydrodynamic size distributions as the nanoparticles increased in size. This change was caused by the oxidation of liquid metal to form elliptically shaped nanoparticles within water, as shown

in the SEM images given in Fig. 2H taken for the nanoparticles 48 hours after production. We found that most of the EGaIn nanoparticles were oxidized, and the obtained EDS spectrum clearly indicates the oxidation of the nanoparticles, as given in Supporting Information S4. Such an oxidation process within the aqueous medium can lead to the formation of GaOOH nanoparticles, and Ga_2O_3 can be obtained after a dehydration and heating process.[6a]

Whilst GaOOH and Ga_2O_3 nanoparticles have application as photocatalysts,[2b,6b,6c] such oxidation process may be disadvantageous for the stability and functionality of EGaIn nanoparticles in aqueous environments when considering biological applications. In order to overcome this limitation, we discovered that nanoparticle oxidation could be inhibited by adding a small amount of trisodium citrate (final concentration of 300 µM) into the final EGaIn colloidal suspensions. Trisodium citrate is widely used as an antioxidant in the food industry with negligible toxicity. The stability of the produced EGaIn nanoparticle suspension was significantly improved (Fig. 2G) and no oxidation was observed, as evidenced by the SEM image taken 48 h after production (Fig. 2I). We further elongated the testing period to 20 days and discovered that the nanoparticle suspension could be readily re-suspended with no oxidation of nanoparticles observed, as shown in Supporting Information S5.

Our strategy for stabilizing the produced EGaIn nanoparticles represents a significant advance in comparison to previous reports that present studies that described the production of EGaIn nanoparticles in ethanol, using thiol-functionalized small molecules for stabilization.[5d,10] In comparison, our method avoids the use of ethanol, which is less favorable for biological applications due to its relatively strong cytotoxicity. Our application of trithiocarbonate groups for nanoparticle anchoring avoids the use of thiol groups that induce unpleasant odors and are

prone to oxidation reactions. In addition, nanoparticles stabilized by steric repulsion between large conjugated molecules (bPEG in this work) are much more stable in biological buffers.

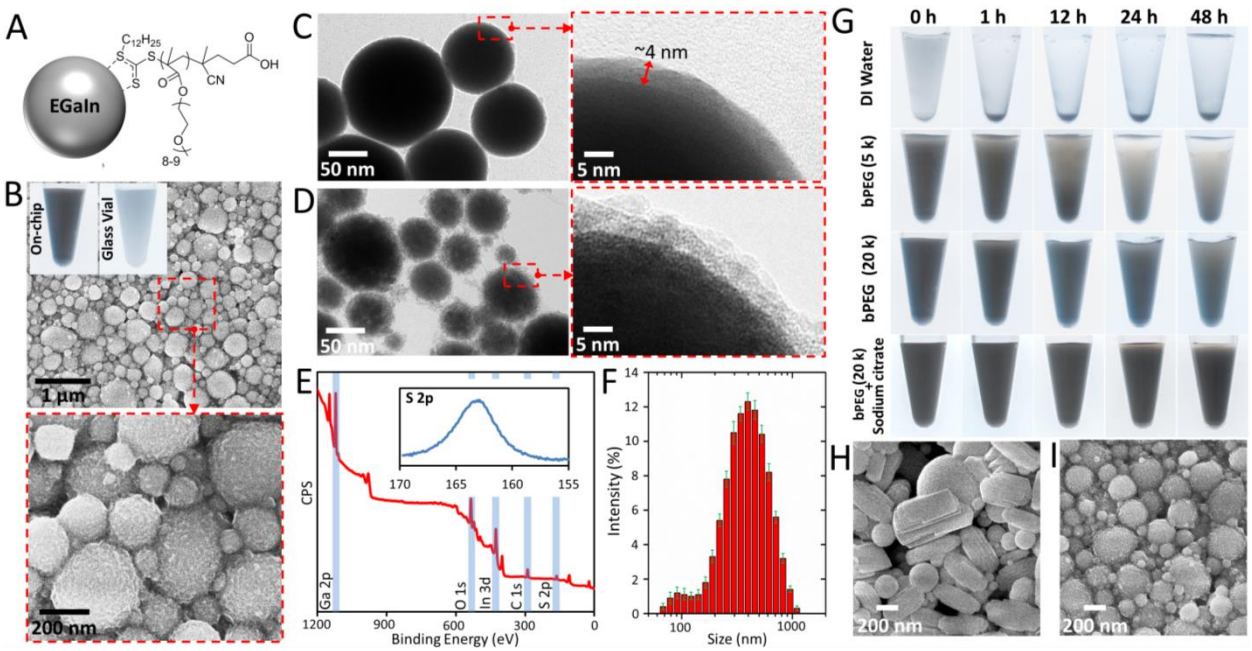

Figure 2. Production of bPEG coated liquid metal nanoparticles. (A) Proposed scheme of the conjugation between bPEG molecules and EGaIn particle. (B) SEM images for the produced EGaIn nanoparticles. TEM images obtained for the EGaIn nanoparticles (C) without and (D) with the use of bPEG. (E) XPS spectrum obtained for bPEG coated nanoparticles, the inset shows the evidence of coating with the presence of 2p peak for sulfur. (F) Hydrodynamic size distribution of the obtained EGaIn nanoparticles. (G) Comparison for the stability of nanoparticles suspensions obtained using different solutions over the duration of 48 hours. SEM images for the nanoparticles (H) without and (I) with the presence of trisodium citrate 48 hours after production.

Following our initial studies on the production mechanism and stability of the EGaIn nanoparticle suspensions in various media, we now describe our work on optimizing the

microfluidic platform to control the nanoparticle size distribution. As depicted in Fig. 1D the EGaIn nanoparticle production originates from the microdroplets disrupted at the T-junction along the microchannel. We hypothesized that smaller size nanoparticles could be produced by increasing the length of the microchannel to enhance the acoustic energy applied to the suspension thereby overcoming surface tension forces. Using the bPEG (MW of 20 kDa) solution with a concentration of 500 μM, we examined this hypothesis by conducting experiments using microchannels with the same *W* and *H* of 5 and 0.05 mm, respectively, but different lengths of 10, 50, and 100 mm. The flow rates of the bPEG solution and EGaIn were set at 50 and 1 μL/min, respectively. The hydrodynamic size *D* distributions generated by these experiments are given in **Figure 3**A, where it is evident that there is a shift in the distribution towards smaller particle sizes when a longer channel was used. The inset of Fig. 3A shows that the average *D* was reduced from ~400 to ~250 nm when *L* was increased from 10 to 100 mm.

We further investigated the effect of the channel width *W* on the size distribution of the nanoparticles. We obtained the distribution, *D*, using microchannels with the same length of 10 mm and different widths of 1, 3 and 7 mm, as shown in Fig. 3B (schematics of the microchannels are given in the insets). We noted two peaks in the distribution (~200 and 700 nm) when a narrow channel of 1 mm was used; the two peaks merged into one after increasing the width *W* of the channel. This phenomenon can be attributed to the fact that liquid metal particles travel slower inside the channel with a larger *W* and therefore, experience more acoustic energy for generating smaller particles. The hydrodynamic size distribution of the nanoparticles can be further controlled using centrifugal force, and we examined this method by centrifuging the suspension with different rotational speeds from 1000 to 3000 RPM for 3 min, as shown in Fig. 3C. We can now see that a narrow distribution of the nanoparticles with the peak shifted towards smaller

sizes could be achieved by increasing the speed from 1000 (corresponding to ~67 g-force) to 3000 RPM (corresponding to ~604 g-force). The insets of Fig. 3C show the obtained suspensions after centrifuging at different speeds, and the yield of EGaIn nanoparticles decreased from ~40 mg at 1000 RPM to ~15 mg at 3000 RPM.

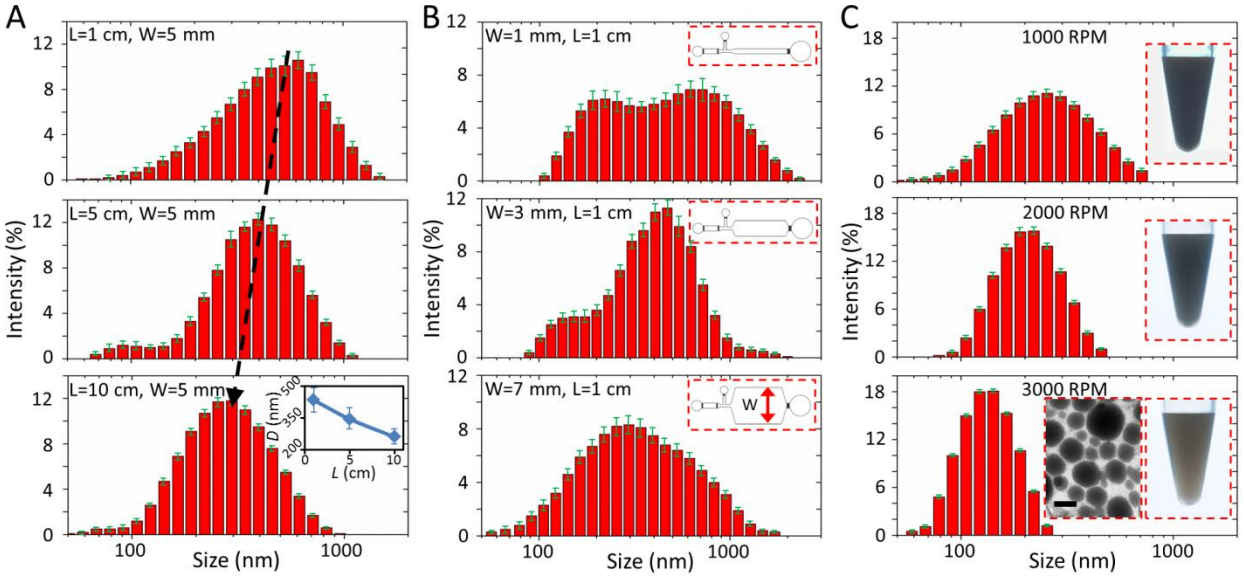

Figure 3. Controlling the size distributions of EGaIn nanoparticles. (A) Hydrodynamic size distributions of EGaIn nanoparticles obtained using microchannels with different lengths *L*, and their average diameters *D* are given in the inset. (B) Hydrodynamic size distributions of EGaIn nanoparticles obtained using microchannels with different widths *W*. The insets show the schematics of the corresponding microchannels used. (C) Hydrodynamic size distributions of EGaIn nanoparticles obtained after separation using a centrifuge rotating at different speeds. The obtained suspensions after separation and the TEM image for the nanoparticles after separating using 3000 RPM are given in the insets. Scale bar is 50 nm.

Surface functionalization is central to any significant advances in the application of nanomaterials, especially in fields such as pharmaceutical and biomedical sciences. To achieve successful functionalization we firstly investigated the galvanic replacement of the surface of EGaIn nanoparticles with silver (Ag). In addition to conventional electronic, photonic, antimicrobial, and disinfectant applications for Ag nanoparticles, research has also shown the emergence of the use of Ag nanoparticles in biomedical applications such as biosensors,[18] photothermal therapy,[19] and drug delivery.[20] The chemical reaction is straightforward that Ga is oxidized in the presence of Ag^+ ions that have a higher reduction potential, and consequently Ag^+ ions will be reduced to the metallic state at the surface of EGaIn. We added 20 µL of EGaIn nanoparticles grafted with bPEG (20 kDa) into 1 mL $AgNO_3$ solution (concentration of 100 µM), and we observed the formation of Ag nanoparticles with a size of ~10 nm on the surface of EGaIn particles, uniformly coating the surface of EGaIn and forming nano-sized liquid metal marbles,[21] as shown in the SEM and TEM images given in **Figure 4**A. We found that the size of the reduced Ag nanoparticles increased to ~50 nm when an $AgNO_3$ solution with a higher concentration of 1000 µM was used, as shown in the SEM and TEM images given in Fig. 4B.

The EDS spectrum for the Ag coated EGaIn nanoparticles produced using different concentrations of $AgNO_3$ are given in Fig. 4C. In principle both Ga and In can be oxidized when in contact with $AgNO_3$, however, since Ga has the lowest standard reduction potential it is more likely to be replaced by Ag^+. This is confirmed by the EDS spectrum, showing the consumption of Ga is more rapid at increased concentrations of $AgNO_3$, which is consistent with previously reported results using bulk Galinstan liquid metal material.[6b] The inset of Fig. 4C shows the obtained EGaIn-Ag nanoparticle suspensions when reacting with $AgNO_3$ solution with concentrations ranging from 10 to 1000 µM. Interestingly, we observed a colour change of the

suspensions from light yellow to dark grey when increasing the concentration of $AgNO_3$. We obtained UV-VIS spectra for these suspensions and the results are given in Supporting Information S6.

We already demonstrated that the coated bPEG molecules are able to stabilize the EGaIn nanoparticles in aqueous media, and we postulated that further bio-functionalization of the nanoparticles could be possible exploiting the presence of carboxyl group on the bPEG chains. We conducted a proof-of-concept experiment to couple fluorophore-labelled antibody to the bPEG grafted EGaIn nanoparticles, as depicted in Fig. 4D, where 1-Ethyl-3-(3-dimethylaminopropyl)carbodiimide (EDC)-mediated crosslinking method was used. In brief, EDC (final concentration of 5 mM) was firstly added into 100 µL of the produced EGaIn nanoparticle suspension to react with carboxylic acid groups on the bPEG to form an active O-acylisourea intermediate. The suspension was washed with DI water 30 min after the reaction and 2 µL of fluorophore labelled anti-rabbit IgG solution (concentration of 2 mg/mL) was added to the washed nanoparticle suspension to allow for the displacement from primary amino groups on the antibodies to form amide bonds with the carboxyl groups on bPEG. The nanoparticles were later washed with DI water several times and we examined the functionalization using a fluorescence spectrophotometer. The obtained emission spectra for the fluorophore labelled antibody solution, bare EGaIn nanoparticle suspension, and antibody-functionalized EGaIn nanoparticle suspension are given in Fig. 4E. The antibody solution has an emission peak at ~600 nm and the presence of such a peak for the spectrum obtained with the antibody-conjugated EGaIn nanoparticle suspension clearly proved the success of functionalization. The insets of Fig. 4E show the bright field and fluorescent images taken by a fluorescent microscope for the dry antibody-functionalized EGaIn nanoparticle cluster, in which we can clearly see the bright

orange-coloured fluorescent light emitted from the nanoparticles. The success of the antibody functionalization is further evidenced by the shifting of the DLS distribution peak towards the larger size by ~20 nm after conjugation, as shown in Supporting Information S9.

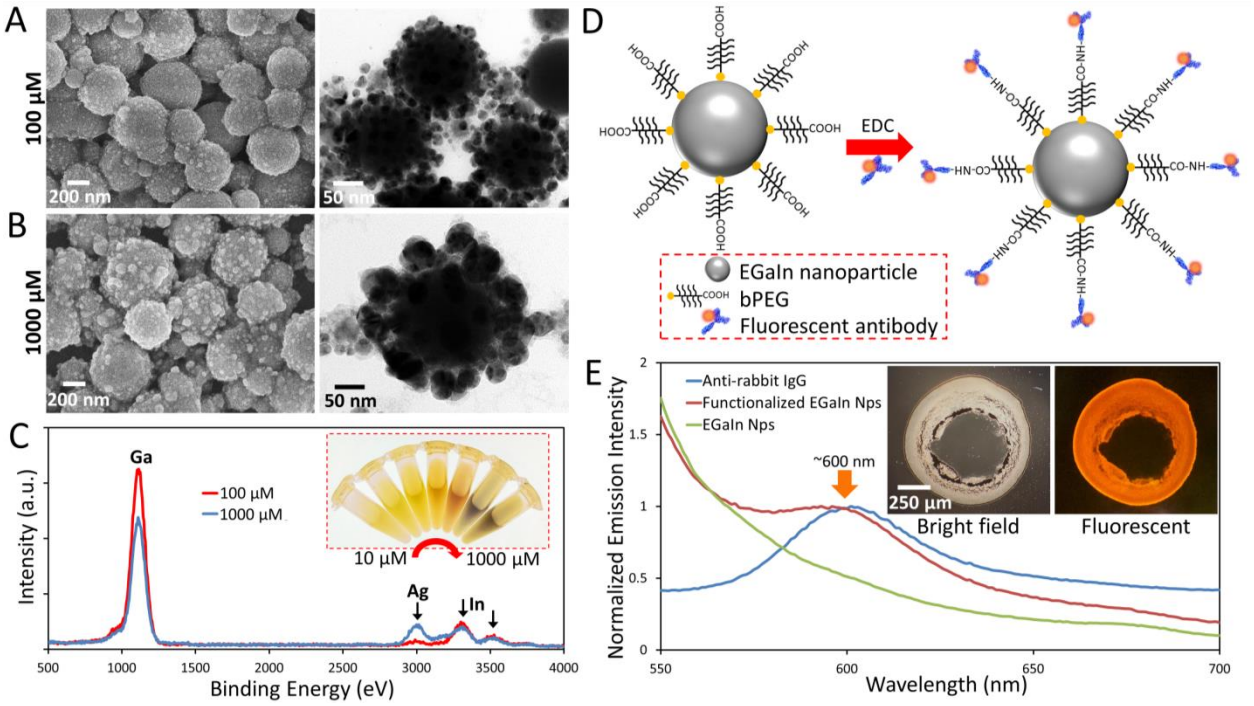

Figure 4. Surface modification of the EGaIn nanoparticles. Coating the surface of EGaIn with Ag nanoparticles after galvanic replacement using $AgNO_3$ solutions with a concentration of (A) 100 and (B) 1000 µM. (C) EDS spectrum measured for the Ag coated EGaIn nanoparticles obtained using different concentrations of $AgNO_3$. The inset shows the image of the obtained suspensions. (D) Functionalization of the bPEG coated EGaIn nanoparticles with fluorophore-labelled antibody molecules. (E) Normalized emission spectrum obtained from fluorescent spectroscopy for the antibody and EGaIn nanoparticles with or without functionalization. The insets show the bright field and fluorescent images taken for a dried nanoparticle suspension cluster.

In summary, we describe a microfluidic-based system for on-chip production of EGaIn liquid metal nanoparticles in aqueous media with a high efficiency using acoustic-wave-induced forces. Such a system is simple and can be readily adapted in any labs equipped with inexpensive ultrasonic baths without the need of conventional bulky and expensive high-power sonication probes. Additionally, the size distributions of the produced EGaIn nanoparticles can be easily tuned by adjusting the dimensions of the microchannels dependent on requirements. Most importantly, we discovered that bPEG polymer with trithiocarbonate groups can be used for grafting the surface of EGaIn liquid metal, forming conjugated systems to stabilize the produced nanoparticles directly in aqueous media. Moreover, we also resolved the issue of previously reported oxidation of liquid metal nanoparticles in water simply by adding a small amount of trisodium citrate into the produced suspension. Based on the excellent results obtained for the production and stabilization of EGaIn nanoparticles, we discovered that the uniqueness of the liquid metal itself allows for the further modification of the surface simply by galvanic replacement with noble metals such as Ag. Furthermore, the grafted bPEG molecules allow for further bio-functionalization by forming amide bond with other desired molecules. Thus, the simplicity and versatility of the developed production platform, together with the functionality of the produced EGaIn nanoparticles, will certainly offer the potential of new opportunities for developing future liquid metal-enabled systems for innovative biomedical applications such as biosensors,[22] and photothermal/electric field induced intracellular delivery.[23]

Experimental Section

Polymer Synthesis: See Supporting Information S1.

Chemicals, Reagents, and Preparation: EGaIn liquid metal, trisodium citrate, DMSA, and $AgNO_3$ powder were purchased from Sigma Aldrich, Australia. The fluorophore conjugated donkey anti-rabbit IgG (ab175470) was purchase from Abcam, USA. The ultrasonic bath (1.3 L, 20 kHz, 65 W) was purchase from JIETAI Manufacture Ltd., China.

Fabrication and Characterization: PDMS microchannels were fabricated using standard photolithography techniques.[2c] SEM images were obtained using a JEOL JSM-7500FA scanning electron microscope. TEM images were obtained using a JEOL JEM-2011 transmission electron microscope. EDS mappings were conducted using JEOL JEM-ARM200f scanning transmission electron microscope. PMMA frames and magnet holder were fabricated using a CO_2 laser engraving system (Versa Laser System, Model VLS3.50, Universal Laser System, Ltd.). A zeta-sizer (Zetasizer Nano ZS, Marvern Instrument, USA) was used to measure the size distribution of the obtained EGaIn nanoparticles. The concentration of the EGaIn nanoparticles was measured by weighing the dried suspensions. UV-VIS spectra was obtained using a UV/VIS Spectrophotometer (Uv-5200Pc, Metash instrument Co., Ltd, China). The fluorescent emission spectra were obtained using a fluorescence spectrophotometer (Cary Eclipse 500, Agilent Technologies, USA).

Supporting Information

Supporting Information is available from the Wiley Online Library.

Acknowledgements

Dr. Shi-Yang Tang is the recipient of the Vice-Chancellor's Postdoctoral Research Fellowship funded by the University of Wollongong. Prof. Tom P. Davis and Dr. Ruirui Qiao are supported by the Australian Research Council Centre of Excellence in Convergent Bio-Nano Science and Technology (project number CE140100036). The authors acknowledge use of the facilities and the assistance of Dr. David Mitchell at the UOW Electron Microscopy Centre.

References

[1] M. D. Dickey, *ACS Appl. Mater. Interfaces* **2014**, *6*, 18369-18379.

[2] a) S.-Y. Tang, K. Khoshmanesh, V. Sivan, P. Petersen, A. P. O'Mullane, D. Abbott, A. Mitchell, K. Kalantar-zadeh, *Proc. Natl. Acad. Sci. U. S. A.* **2014**, *111*, 3304-3309; b) S.-Y. Tang, V. Sivan, P. Petersen, W. Zhang, P. D. Morrison, K. Kalantar- zadeh, A. Mitchell, K. Khoshmanesh, *Adv. Funct. Mater.* **2014**, *24*, 5851-5858; c) S. Y. Tang, J. Zhu, V. Sivan, B. Gol, R. Soffe, W. Zhang, A. Mitchell, K. Khoshmanesh, *Adv. Funct. Mater.* **2015**, *25*, 4445-4452; d) K. Khoshmanesh, S.-Y. Tang, J. Y. Zhu, S. Schaefer, A. Mitchell, K. Kalantar-Zadeh, M. D. Dickey, *Lab Chip* **2017**, *17*, 974-993; e) J. Zhang, Y. Yao, L. Sheng, J. Liu, *Adv. Mater.* **2015**, *27*, 2648-2655.

[3] a) M. D. Dickey, *Adv. Mater.* **2017**; b) C. B. Cooper, K. Arutselvan, Y. Liu, D. Armstrong, Y. Lin, M. R. Khan, J. Genzer, M. D. Dickey, *Adv. Funct. Mater.* **2017**, *27*; c) T. Lu, E. Markvicka, Y. Jin, C. Majidi, *ACS Appl. Mater. Interfaces* **2017**; d) Q. Wang, Y. Yu, J. Yang, J. Liu, *Adv. Mater.* **2015**, *27*, 7109-7116.

[4] a) X. Wang, J. Zhuang, Q. Peng, Y. Li, *Nature* **2005**, *437*, 121-124; b) P. Zhao, N. Li, D. Astruc, *Coord. Chem. Rev.* **2013**, *257*, 638-665.

[5] a) S.-Y. Tang, I. D. Joshipura, Y. Lin, K. Kalantar- Zadeh, A. Mitchell, K. Khoshmanesh, M. D. Dickey, *Adv. Mater.* **2016**, *28*, 604-609; b) Y. Lin, C. Cooper, M. Wang, J. J. Adams, J. Genzer, M. D. Dickey, *Small* **2015**, *11*, 6397-6403; c) S. Y. Tang, B. Ayan, N. Nama, Y. Bian, J. P. Lata, X. Guo, T. J. Huang, *Small* **2016**, *12*, 3861-3869; d) Y. Lu, Q. Hu, Y. Lin, D. B. Pacardo, C. Wang, W. Sun, F. S. Ligler, M. D. Dickey, Z. Gu, *Nat. Commun.* **2015**, *6*, 10066; e) Y. Lin, Y. Liu, J. Genzer, M. D. Dickey, *Chem. Sci.* **2017**, *8*, 3832-3837.

[6] a) N. Syed, A. Zavabeti, M. Mohiuddin, B. Zhang, Y. Wang, R. S. Datta, P. Atkin, B. J. Carey, C. Tan, J. van Embden, *Adv. Funct. Mater.* **2017**, *27*; b) F. Hoshyargar, J. Crawford, A. P. O'Mullane, *J. Am. Chem. Soc.* **2016**, *139*, 1464-1471; c) W. Zhang, J. Z. Ou, S.-Y. Tang, V. Sivan, D. D. Yao, K. Latham, K. Khoshmanesh, A. Mitchell, A. P. O'Mullane, K. Kalantar- zadeh, *Adv. Funct. Mater.* **2014**, *24*, 3799-3807.

[7] a) S. A. Chechetka, Y. Yu, X. Zhen, M. Pramanik, K. Pu, E. Miyako, *Nat. Commun.* **2017**, *8*, 15432; b) Y. Lu, Y. Lin, Z. Chen, Q. Hu, Y. Liu, S. Yu, W. Gao, M. D. Dickey, Z. Gu, *Nano Lett.* **2017**, *17*, 2138-2145.

[8] a) I. D. Tevis, L. B. Newcomb, M. Thuo, *Langmuir* **2014**, *30*, 14308-14313; b) S. Çınar, I. D. Tevis, J. Chen, M. Thuo, *Sci. Rep.* **2016**, *6*, 21864.

[9] J. Ma, S. M.-Y. Lee, C. Yi, C.-W. Li, *Lab Chip* **2017**, *17*, 209-226.

[10] L. R. Finkenauer, Q. Lu, I. F. Hakem, C. Majidi, M. R. Bockstaller, *Langmuir* **2017**, *33*, 9703-9710.

[11] A. Kraynov, T. E. Müller (2011) Concepts for the stabilization of metal nanoparticles in ionic liquids. Applications of Ionic Liquids in Science and Technology: InTech.

[12] C. Boyer, V. Bulmus, T. P. Davis, V. Ladmiral, J. Liu, S. Perrier, *Chem. Rev.* **2009**, *109*, 5402-5436.

[13] a) I. Banerjee, R. C. Pangule, R. S. Kane, *Adv. Mater.* **2011**, *23*, 690-718; b) T. Blin, A. Kakinen, E. H. Pilkington, A. Ivask, F. Ding, J. F. Quinn, M. R. Whittaker, P. C. Ke, T. P. Davis, *Polym. Chem.* **2016**, *7*, 1931-1944.

[14] J. M. Ren, T. G. McKenzie, Q. Fu, E. H. Wong, J. Xu, Z. An, S. Shanmugam, T. P. Davis, C. Boyer, G. G. Qiao, *Chem. Rev.* **2016**, *116*, 6743-6836.

[15] a) J. W. Hotchkiss, A. B. Lowe, S. G. Boyes, *Chem. Mater.* **2007**, *19*, 6-13; b) B. Ebeling, P. Vana, *Macromolecules* **2013**, *46*, 4862-4871.

[16] Z. J. Farrell, C. Tabor, *Langmuir* **2017**.

[17] H. M. Zareie, C. Boyer, V. Bulmus, E. Nateghi, T. P. Davis, *Acs Nano* **2008**, *2*, 757-765.

[18] a) A. F. Chrimes, K. Khoshmanesh, S.-Y. Tang, B. R. Wood, P. R. Stoddart, S. S. Collins, A. Mitchell, K. Kalantar-zadeh, *Biosens. Bioelectron.* **2013**, *49*, 536-541; b) B. H. Jun, M. S. Noh, J. Kim, G. Kim, H. Kang, M. S. Kim, Y. T. Seo, J. Baek, J. H. Kim, J. Park, *Small* **2010**, *6*, 119-125.

[19] G. B. Braun, T. Friman, H.-B. Pang, A. Pallaoro, T. H. De Mendoza, A.-M. A. Willmore, V. R. Kotamraju, A. P. Mann, Z.-G. She, K. N. Sugahara, *Nat. Mater.* **2014**, *13*, 904.

[20] J. Shi, L. Wang, J. Zhang, R. Ma, J. Gao, Y. Liu, C. Zhang, Z. Zhang, *Biomaterials* **2014**, *35*, 5847-5861.

[21] V. Sivan, S.-Y. Tang, A. P. O'Mullane, P. Petersen, N. Eshtiaghi, K. Kalantar- zadeh, A. Mitchell, *Adv. Funct. Mater.* **2013**, *23*, 144-152.

[22] a) J. Guo, X. Huang, Y. Ai, *Anal. Chem.* **2015**, *87*, 6516-6519; b) J. Guo, *Anal. Chem.* **2017**, *89*, 8609-8613.

[23] M. P. Stewart, A. Sharei, X. Ding, G. Sahay, R. Langer, K. F. Jensen, *Nature* **2016**, *538*, 183-192.